J|A|C|S
ARTICLES
Published on Web 02/02/2008

$B_2(BO)_2^{2-}$ — Diboronyl Diborene: A Linear Molecule with a Triple Boron−Boron Bond

Si-Dian Li,*[,†,‡] Hua-Jin Zhai,[§,||] and Lai-Sheng Wang*[,§,||]

Institute of Molecular Sciences, Shanxi University, Taiyuan 030006, People's Republic of China, Xinzhou Teachers' University, Xinzhou 034000, Shanxi, People's Republic of China, Department of Physics, Washington State University, 2710 University Drive, Richland, Washington 99354, and Chemical and Materials Sciences Division, Pacific Northwest National Laboratory, MS K8-88, P.O. Box 999, Richland, Washington 99352

Received September 13, 2007; E-mail: lisidian@yahoo.com; ls.wang@pnl.gov

Abstract: We have produced and investigated an unique boron oxide cluster, $B_4O_2^-$, using photoelectron spectroscopy and *ab initio* calculations. Relatively simple and highly vibrationally resolved PES spectra were obtained at two photon energies (355 and 193 nm). The electron affinity of neutral B_4O_2 was measured to be 3.160 ± 0.015 eV. Two excited states were observed for B_4O_2 at excitation energies of 0.48 and 0.83 eV above the ground state. Three vibrational modes were resolved in the 355 nm spectrum for the ground state of B_4O_2 with frequencies of 350 ± 40, 1530 ± 30, and 2040 ± 30 cm^{-1}. *Ab initio* calculations showed that neutral B_4O_2 ($D_{\infty h}$, $^3\Sigma_g^-$) and anionic $B_4O_2^-$ ($D_{\infty h}$, $^2\Pi_u$) both possess highly stable linear structures (O≡B−B═B−B≡O), which can be viewed as a B_2 dimer bonded to two terminal boronyl groups. The lowest nonlinear structures are at least 1.5 eV higher in energy. The calculated electron detachment energies from the linear $B_4O_2^-$ and the vibrational frequencies agree well with the experimental results. The three observed vibrational modes are due to the B−B, B═B, and B≡O symmetric stretching vibrations, respectively, in the linear $B_2(BO)_2$. Chemical bonding analyses revealed that the HOMO of $B_2(BO)_2$, which is half-filled, is a bonding π orbital in the central B_2 unit. Thus, adding two electrons to $B_2(BO)_2$ leads to a B≡B triple bond in $[O{\equiv}B{-}B{\equiv}B{-}B{\equiv}O]^{2-}$. Possibilities for stabilizing $B_2(BO)_2^{2-}$ in the form of $B_2(BO)_2Li_2$ are considered computationally and compared with other valent isoelectronic, triple bonded species, $B_2H_2Li_2$, $B_2H_2^{2-}$, and C_2H_2. The high stability of $B_2(BO)_2^{2-}$ suggests that it may exist as a viable building block in the condensed phase.

1. Introduction

Boron is an electron-deficient element and possesses interesting chemical bonding properties.[1,2] The chemical bonding in boranes[3] and, more recently, in elemental boron clusters[4−6] is dominated by three-center two-electron bonds and aromaticity/antiaromaticity. Boron−boron multiple bonds are rare due to boron's electron deficiency but have been studied both experimentally[7−13] and theoretically.[14−17] Partial BB π-bonding was induced through one-electron reduction of a B_2R_4 precursor.[7,8] Further reduction led to a $B_2R_4^{2-}$ dianion with the first reported B═B double bond (1.62−1.64 Å) in 1992.[9] The diborene B_2H_2 is probably the simplest molecule with a B═B

† Shanxi University.
‡ Xinzhou Teachers' University.
§ Washington State University.
|| Pacific Northwest National Laboratory.

(1) Greenwood, N. N.; Earnshaw, A. *Chemistry of the Elements*, 2nd ed.; Butterworth-Heinemann: Oxford, 1997.
(2) Cotton, F. A.; Wilkinson, G.; Murrillo, C. A.; Bochmann, M. *Advanced Inorganic Chemistry*, 6th ed.; John Wiley & Sons: New York, 1999.
(3) (a) Lipscomb, W. N. *Boron Hydrides*; Benjamin: New York, 1963. (b) Lipscomb, W. N. *Science* **1977**, *196*, 1047.
(4) (a) Hanley, L.; Whitten, J. L.; Anderson, S. L. *J. Phys. Chem.* **1988**, *92*, 5803. (b) Kato, H.; Yamashita, K.; Morokuma, K. *Chem. Phys. Lett.* **1992**, *190*, 361. (c) Martin, J. M. L.; Francois, J. P.; Gijbels, R. *Chem. Phys. Lett.* **1992**, *189*, 529. (d) Kawai, R.; Weare, J. H. *Chem. Phys. Lett.* **1992**, *191*, 311. (e) Boustani, I. *Int. J. Quantum Chem.* **1994**, *52*, 1081. (f) Ricca, A.; Bauschlicher, C. W. Jr. *Chem. Phys.* **1996**, *208*, 233. (g) Boustani, I. *Phys. Rev. B* **1997**, *55*, 16426. (h) Gu, F. L.; Yang, X. M.; Tang, A. C.; Jiao, H. J.; Schleyer, P. v. R. *J. Comput. Chem.* **1998**, *19*, 203. (i) Fowler, J. E.; Ugalde, J. M. *J. Phys. Chem. A* **2000**, *104*, 397. (j) Aihara, J. I.; Kanno, H.; Ishida, T. *J. Am. Chem. Soc.* **2005**, *127*, 13324.
(5) (a) Zhai, H. J.; Wang, L. S.; Alexandrova, A. N.; Boldyrev, A. I. *J. Chem. Phys.* **2002**, *117*, 7917. (b) Zhai, H. J.; Alexandrova, A. N.; Birch, K. A.; Boldyrev, A. I.; Wang, L. S. *Angew. Chem., Int. Ed.* **2003**, *42*, 6004. (c) Zhai, H. J.; Kiran, B.; Li, J.; Wang, L. S. *Nat. Mater.* **2003**, *2*, 827. (d) Zhai, H. J.; Wang, L. S.; Zubarev, D. Y.; Boldyrev, A. I. *J. Phys. Chem. A* **2006**, *110*, 1689.
(6) For a recent review on all-boron aromatic clusters, see: Alexandrova, A. N.; Boldyrev, A. I.; Zhai, H. J.; Wang, L. S. *Coord. Chem. Rev.* **2006**, *250*, 2811.
(7) (a) Klusik, H.; Berndt, A. *Angew. Chem., Int. Ed. Engl.* **1981**, *20*, 870. (b) Berndt, A.; Klusik, H.; Schluter, K. *J. Organomet. Chem.* **1981**, *222*, C25.
(8) (a) Grigsby, W. J.; Power, P. P. *Chem. Commun.* **1996**, *19*, 2235. (b) Grigsby, W. J.; Power, P. P. *Chem.—Eur. J.* **1997**, *3*, 368.
(9) (a) Moezzi, A.; Olmstead, M. M.; Power, P. P. *J. Am. Chem. Soc.* **1992**, *114*, 2715. (b) Moezzi, A.; Bartlett, R. A.; Power, P. P. *Angew. Chem., Int. Ed. Engl.* **1992**, *31*, 1082.
(10) Noth, H.; Knizek, J.; Ponikwar, W. *Eur. J. Inorg. Chem.* **1999**, *11*, 1931.
(11) Tague, T. J., Jr.; Andrews, L. *J. Am. Chem. Soc.* **1994**, *116*, 4970.
(12) Knight, L. B., Jr.; Kerr, K.; Miller, P. K.; Arrington, C. A. *J. Phys. Chem.* **1995**, *99*, 16842.
(13) Zhou, M.; Tsumori, N.; Li, Z.; Fan, K.; Andrews, L.; Xu, Q. *J. Am. Chem. Soc.* **2002**, *124*, 12936.
(14) (a) Dill, J. D.; Schleyer, P. v. R.; Pople, J. A. *J. Am. Chem. Soc.* **1975**, *97*, 3402. (b) Kaufmann, E.; Schleyer, P. v. R. *Inorg. Chem.* **1988**, *27*, 3987.
(15) Jouany, C.; Barthelat, J. C.; Daudey, J. P. *Chem. Phys. Lett.* **1987**, *136*, 52.
(16) Treboux, G.; Barthelat, J. C. *J. Am. Chem. Soc.* **1993**, *115*, 4870.
(17) (a) Armstrong, D. R. *Theor. Chim. Acta* **1981**, *60*, 159. (b) Sana, M.; Leroy, G.; Henriet, C. *THEOCHEM* **1989**, *187*, 233. (c) Peric, M.; Ostojic, B.; Engels, B. *J. Mol. Spect.* **1997**, *182*, 280.

double bond, and it was characterized via ESR spectroscopy in inert matrices at 4 K in 1995,[12] constituting the simplest tetraatomic radical with a triplet ($^3\Sigma_g^-$) ground state. A boron−boron triple bond is extremely rare, which was first reported by Zhou et al. in 2002.[13,18] They observed a linear molecule OCBBCO in an argon matrix at 8 K and showed that it possesses some boron−boron triple bond character.

Boron does form a strong triple bond with oxygen in the diatomic BO molecule (boronyl), which is isoelectronic with CN. Boronyl is known as a σ-radical[19−21] and was speculated to exist as network terminals in liquid B_2O_3 at high temperatures.[22] However, the chemistry of boronyl is relatively unknown, in contrast to CN, which is an important inorganic ligand. The electronic structure and bond strength of BO are similar to those of CN,[20,21] suggesting that it may be a robust chemical unit and may maintain its structural integrity in certain chemical compounds. Boron oxide clusters are important species relevant to the development of highly energetic boron-based propellants.[23] But our knowledge about these species is surprisingly limited beyond the BO molecule.[24] We are interested in characterizing the electronic structure and chemical bonding of boron oxide clusters using photoelectron spectroscopy (PES) and theoretical calculations.[21,25] In a recent communication, we reported a PES and density-functional theory (DFT) study of two boron oxide clusters, $B_3O_2^-$ and $B_4O_3^-$. They are found surprisingly to possess a linear $B(BO)_2^-$ ($D_{\infty h}$,$^3\Sigma_g$) and triangular $B(BO)_3^-$ (D_{3h}, $^2A_2''$) structure, which can be viewed as two and three boronyls bonded to a single B atom. A few previous studies relevant to BO chemistry are available in the literature.[18,26−29] We showed previously that in Au_nBO^- ($n = 1-3$) clusters BO behaves like a monovalent structural unit in its bonding to Au.[26] Theoretical calculations by one of us suggested that carbon boronyls $(CBO)_n$ ($n = 3-7$) are stable species.[27] Schwarz and co-workers observed C_nBO ($n = 2, 4$) in gas-phase mass spectrometric experiments.[28] Zhou et al.[18] observed two boronyl species OBBCCO and OBCCBO in a low-temperature matrix upon photolysis of the OCBBCO molecule.[13]

In the current contribution, we report a combined PES and theoretical investigation of a new boron oxide cluster, $B_4O_2^-$, which exhibits both boron−boron multiple bonding and structural features of boronyls. We produced the $B_4O_2^-$ cluster using laser vaporization and obtained its PES spectra at 355 nm (3.496 eV) and 193 nm (6.424 eV) photon energies. The 355 nm spectrum was vibrationally resolved, revealing three vibrational modes with frequencies of 350 ± 40, 1530 ± 30, and 2040 ± 30 cm^{-1}. An accurate electron affinity of 3.160 ± 0.015 eV was obtained for the B_4O_2 neutral. Extensive DFT and *ab initio* calculations were performed for B_4O_2 and $B_4O_2^-$, which were found to possess highly stable linear structures, O≡B−B═B−B≡O for B_4O_2 ($D_{\infty h}$,$^3\Sigma_g^-$) and $[O{\equiv}B{-}B{=}B{-}B{\equiv}O]^-$ ($D_{\infty h}$,$^2\Pi_u$) for $B_4O_2^-$. These structures are confirmed by the excellent agreement between the calculated electron detachment energies and vibrational frequencies and the experimental results. Molecular orbital (MO) and bond order analyses showed that the B═B bond in $B_4O_2^-$ is of the order 2.5. Addition of one more electron to $B_4O_2^-$ leads to a unprecedented closed-shell, triple bonded B_2 species, $[O{\equiv}B{-}B{\equiv}B{-}B{\equiv}O]^{2-}$ ($D_{\infty h}$,$^1\Sigma_g^+$), i.e., diboronyl diborene.

2. Experimental and Computational Methods

2.1. Photoelectron Spectroscopy. The experiment was carried out using a magnetic-bottle-type PES apparatus equipped with a laser vaporization supersonic cluster source, details of which have been described previously.[30,31] Briefly, the boron oxide cluster anions were produced by laser vaporization of a pure disk target made of enriched ^{10}B isotope (99.75%) in the presence of a helium carrier gas seeded with 0.01% O_2. The resulting $B_mO_n^-$ clusters were analyzed using a time-of-flight mass spectrometer. The $B_4O_2^-$ cluster of current interest was mass-selected and decelerated before being photodetached. Two detachment photon energies were used in the current experiment: 355 nm (3.496 eV) and 193 nm (6.424 eV). Photoelectrons were collected at nearly 100% efficiency by the magnetic bottle and analyzed in a 3.5 m long electron flight tube. The PES spectra were calibrated using the known spectra of Cu^- and Au^-, and the energy resolution of the apparatus was $\Delta Ek/Ek$ ~2.5%, i.e., ~25 meV for 1 eV electrons.

2.2. Computational Methods. Structural optimizations were accomplished at three theoretical levels, DFT-B3LYP,[32] DFT-B3PW9,[33] and MP2(full)[34] with the augmented Dunning's all-electron basis (aug-cc-pvtz) implemented in the Gaussian 03 program.[35] A variety of initial structures were optimized in search of the ground state structures of B_4O_2, $B_4O_2^-$, $B_4O_2^{2-}$, and $B_2(BO)_2Li_2$. Frequency calculations were done to confirm that all obtained ground state structures are true minima. Vertical one-electron detachment energies were calculated at the OVGF-(full) level[36] using the aug-cc-pvtz basis set at the anion ground state geometries for $B_4O_2^-$. All calculations were carried out using Gaussian 03.[35]

We also calculated the electron detachment energies using the CASPT2 method (complete active-space second-order perturbation theory)[37] using the aug-cc-pvtz basis set, based on the optimized structures at the B3LYP/aug-cc-pvtz level. The CASPT2(5, 6) (with five electrons and six orbitals forming the active space) and CASPT2-

(18) Zhou, M.; Jiang, L.; Xu, Q. *Chem.—Eur. J.* **2004**, *10*, 5817.
(19) Huber, K. P.; Herzberg, G. *Constants of Diatomic Molecules*; Van Nostrand Reinhold: New York, 1979.
(20) Pyykko, P. *Mol. Phys.* **1989**, *67*, 871.
(21) Zhai, H. J.; Wang, L. M.; Li, S. D.; Wang, L. S. *J. Phys. Chem. A* **2007**, *111*, 1030.
(22) Mackenzie, J. D. *J. Phys. Chem.* **1959**, *63*, 1875.
(23) Bauer, S. H. *Chem. Rev.* **1996**, *96*, 1907.
(24) (a) Weltner, W., Jr.; Warn, J. R. W. *J. Chem. Phys.* **1962**, *37*, 292. (b) Sommer, A.; White, D.; Linevsky, M. J.; Mann, D. E. *J. Chem. Phys.* **1963**, *38*, 87. (c) Ruscic, B. M.; Curtiss, L. A.; Berkowitz, J. *J. Chem. Phys.* **1984**, *80*, 3962. (d) Doyle, R. J., Jr. *J. Am. Chem. Soc.* **1988**, *110*, 4120. (e) Hanley, L.; Anderson, S. L. *J. Chem. Phys.* **1988**, *89*, 2848. (f) Burkholder, T. R.; Andrews, L. *J. Chem. Phys.* **1991**, *95*, 8697. (g) Nemukhin, A. V.; Weinhold, F. *J. Chem. Phys.* **1993**, *98*, 1329. (h) Peiris, D.; Lapicki, A.; Anderson, S. L.; Napora, R.; Linder, D.; Page, M. *J. Phys. Chem. A* **1997**, *101*, 9935.
(25) Zhai, H. J.; Li, S. D.; Wang, L. S. *J. Am. Chem. Soc.* **2007**, *129*, 9254.
(26) Zubarev, D. Yu.; Boldyrev, A. I.; Li, J.; Zhai, H. J.; Wang, L. S. *J. Phys. Chem. A* **2007**, *111*, 1648.
(27) (a) Li, S. D.; Miao, C. Q.; Guo, J. C.; Ren, G. M. *J. Comput. Chem.* **2005**, *26*, 799. (b) Ren, G. M.; Li, S. D.; Miao, C. Q. *THEOCHEM* **2006**, *770*, 193.
(28) (a) McAnoy, A. M.; Dua, S.; Schroder, D.; Bowie, J. H.; Schwarz, H. *J. Phys. Chem. A* **2003**, *107*, 1181. (b) McAnoy, A. M.; Dua, S.; Schroder, D.; Bowie, J. H.; Schwarz, H. *J. Phys. Chem. A* **2004**, *108*, 2426.
(29) Drummond, M. L.; Meunier, V.; Sumpter, B. G. *J. Phys. Chem. A* **2007**, *111*, 6539.
(30) Wang, L. S.; Cheng, H. S.; Fan, J. *J. Chem. Phys.* **1995**, *102*, 9480.
(31) Wang, L. S.; Wu, H. In *Advances in Metal and Semiconductor Clusters Vol. 4 Cluster Materials*; Duncan, M. A., Ed.; JAI Press: Greenwich, CT, 1998; pp 299−343.
(32) (a) Becke, A. D. *J. Chem. Phys.* **1993**, *98*, 5648. (b) Lee, C.; Yang, W.; Parr, R. G. *Phys. Rev. B* **1988**, *37*, 785.
(33) Burke, K.; Perdew, J. P.; Wang, Y. In *Electronic Density Functional Theory: Recent Progress and New Directions*; Dobson, J. F., Vignale, G., Das, M. P., Eds.; Plenum: New York, 1998.
(34) (a) Head-Gordon, M.; Pople, J. A.; Frisch, M. J. *Chem. Phys. Lett.* **1988**, *153*, 503. (b) Head-Gordon, M.; Head-Gordon, T. *Chem. Phys. Lett.* **1994**, *220*, 122.
(35) Frisch, M. J., et al. *Gaussian 03*, revision, A. 1.; Gaussian, Inc.: Pittsburgh, PA, 2003.
(36) (a) von Niessen, W.; Schirmer, J.; Cederbaum, L. S. *Comput. Phys. Rep.* **1984**, *1*, 57. (b) Ortiz, J. V.; Zakrzewski, V. G.; Dolgounircheva, O. In *Conceptual Perspectives in Quantum Chemistry*; Calais, J.-L., Kryachko, E. S., Eds.; Kluwer Academic: Dordrecht, 1997; pp 465−518. (c) Ortiz, J. V. *Adv. Quantum Chem.* **1999**, *35*, 33.

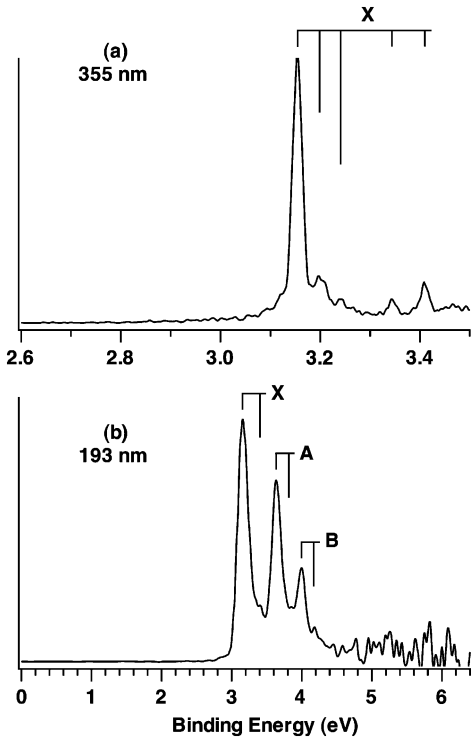

Figure 1. Photoelectron spectra of $B_4O_2^-$ at (a) 355 nm (3.496 eV) and (b) 193 nm (6.424 eV). Vertical bars represent resolved vibrational structures. Three vibrational modes were resolved for the ground state in the 355 nm spectrum (a).

(4, 6) methods were used for $B_4O_2^-$ and B_4O_2, respectively. The calculations were done using the MOLPRO program.[38]

3. Experimental Results

The PES spectra of $B_4O_2^-$ at 355 and 193 nm are shown in Figure 1. Three well-resolved bands were observed at 193 nm at VDEs of 3.16 eV (X), 3.64 eV (A), and 3.99 eV (B). At 355 nm, the ground state transition (X) was resolved into five vibronic peaks. The intense peak at 3.160 eV represents the 0−0 transition and yields an accurate electron affinity for neutral B_4O_2, 3.160 ± 0.015 eV. The other weaker peaks represent vibrational excitations in three vibrational modes, as shown in Figure 1a, with frequencies of 350 (40), 1530 (30), and 2040 (30) cm^{-1}. The 2040 cm^{-1} mode for band X was also partially resolved in the 193 nm (Figure 1b). In fact, vibrational features were also discernible for bands A and B in the 193 nm spectrum, with a frequency of ∼1550 cm^{-1} for both bands. No prominent PES features were observed beyond band B, suggesting that the next higher detachment channel is probably located above 6.4 eV. The observed electron binding energies and vibrational frequencies are given in Tables 1 and 2, where they are compared with computational data.

The PES spectra of $B_4O_2^-$ are quite special in several aspects. First, the sharp 0−0 transition in the ground state band suggests that there are very small structural changes between the ground states of the anion and neutral. Second, the observation of three vibrational modes is remarkable, indicating that the $B_4O_2^-$ cluster and its neutral may have relatively high symmetry. Finally, the neutral B_4O_2 cluster possesses an even number of electrons. However, the PES spectra did not reveal a HOMO−LUMO gap, suggesting that it does not have a closed-shell electron configuration; i.e., the B_4O_2 cluster may possess a triplet ground state.

4. Computational Results

We optimized the structures for B_4O_2 in three charge states, 0, −1, and −2. Figure 2 presents the symmetries, electronic states, relative energies (in bold), minimum vibrational frequencies, and number of imaginary frequencies (in parenthesis) for the optimized structures for all three charge states together. Note the first symbol or number in the label in each case is for B_4O_2, the second, for $B_4O_2^-$, and the third, for $B_4O_2^{2-}$.

Extensive structural searches were done for B_4O_2 by starting from the well-established rhombic B_4 cluster.[39] We first attached the two O atoms terminally, but optimization of this initial structure produced a transition state D_{2h} (^1A_g) (Figure 2 g) with one imaginary frequency. Following this imaginary frequency, we reached a distorted three-dimensional butterfly structure, C_{2v} ($^1A_1$) (Figure 2e), which is a minimum on the potential energy surface. By bridging the two O atoms to the rhombic B_4 cluster with different atomic positions, we obtained three structures: C_{2v} ($^1A_1$) (Figure 2b), C_{2h} (^1A_g) (Figure 2d), and D_2 (^1A) (Figure 2f). The C_{2v} and C_{2h} structures are in fact minima, whereas the D_2 structure is a transition state. Among other structures that we considered, the three-dimensional bicapped D_{4h} (^1A_g) structure (Figure 2h) is a third-order stationary point; and the C_{2v} ($^1A_1$) structure (Figure 2c), which involves a triangular B_3 and a linear BO_2 (ref 21) unit, is a second-order stationary point. The perfectly linear OBBBBO ($D_{\infty h}$, $^3\Sigma_g^-$) structure (Figure 2a) turns out to be the clear global minimum for the B_4O_2 system, which is 1.49 eV lower in energy than the closest isomer (Figure 2b). A similar structure was also reported for B_4O_2 in a recent DFT study.[29]

The same sets of structures were optimized for $B_2(BO)_2^-$ and $B_2(BO)_2^{2-}$ (Figure 2). Very surprisingly, the linear $D_{\infty h}$ structure (Figure 2a) represents the only true minimum on the potential energy surfaces for both the −1 and −2 charge states. All other structures possess at least one imaginary frequency (Figure 2b−h). We further optimized the linear ground state geometries for $B_4O_2^{0/-/2-}$ at several levels of theory (B3LYP, B3PW91, and MP2), as compared in Figure 3. Their Cartesian coordinates at the B3LYP level are given in Table S1 in the Supporting Information. At the B3LYP level, the expectation values of $\langle S^2 \rangle$ were 2.005, 0.7523, and 0.00 for $B_4O_2^{0/-/2-}$, consistent with their triplet, doublet, and singlet spin states.

To assess the stability of $B_2(BO)_2^{2-}$, we also computed a neutral ion pair, $B_2(BO)_2Li_2$ at the B3LYP level. It possesses a D_{2h} (^1A_g) structure with very little distortion to the linear $B_2(BO)_2^{2-}$ core, as shown in Figure 4a, where a valent isoelectronic $B_2H_2Li_2$ species, D_{2h} (^1A_g) (Figure 4b) and C_{2v} ($^1A_1$) (Figure 4c) are also shown. Alternative valent isoelectronic species, $B_2H_2^{2-}$ ($D_{\infty h}$,$^1\Sigma_g^+$) and C_2H_2 ($D_{\infty h}$,$^1\Sigma_g^+$), were also optimized at the same level of theory, as shown in Figure 4d and e, respectively.

The ADE and VDE for the global minimum $B_2(BO)_2^-$ anion were calculated at B3LYP, B3PW91, MP2, CCSD(T)/aug-cc-

(37) (a) Werner, H.-J.; Knowles, P. J. *J. Chem. Phys.* **1985**, *82*, 5053. (b) Knowles, P. J.; Werner, H.-J. *Chem. Phys. Lett.* **1985**, *115*, 259. (c) Werner, H.-J. *Mol. Phys.* **1996**, *89*, 645.
(38) *MOLPRO*, version 2006.1, a package of ab initio programs, Werner, H.-J.; Knowles, P. J.; Lindh, R.; Manby, F. R.; Schütz, M., and others; see http://www.molpro.net.
(39) Zhai, H. J.; Wang, L. S.; Alexandrova, A. N.; Boldyrev, A. I.; Zakrzewski, V. G. *J. Phys. Chem. A* **2003**, *107*, 9319.

Table 1. Observed Ground State Adiabatic and Vertical Detachment Energies (ADE and VDE; in eV) and Vibrational Frequencies from the Photoelectron Spectra of $B_4O_2^-$, Compared to the Corresponding Calculated Values at Several Levels of Theory

	transition[a]/mode[b]	expt[c]	B3LYP	B3PW91	MP2	CCSD(T)	CASPT2
ADE (eV)	$^3\Sigma_g^- \leftarrow {}^2\Pi_u$	3.160 (15)[d]	3.119	3.066	3.082	3.088	3.034
VDE (eV)		3.160 (15)	3.169	3.116	3.120	3.131	3.061
ν_{B-B} (cm^{-1})	σ_g	350 (40)	399	398	408		
$\nu_{B=B}$ (cm^{-1})	σ_g	1530 (30)	1480	1478	1508		
$\nu_{B\equiv O}$ (cm^{-1})	σ_g	2040 (30)	2001	2010	1982		

[a] Refer to the detachment transition from the ground state of the anion to that of the neutral. [b] Refer to the totally symmetric vibrational modes (σ_g) of neutral B_4O_2. [c] Numbers in parentheses represent experimental uncertainties in the last digits. [d] Electron affinity of the B_4O_2 neutral.

Table 2. Experimental Electron Detachment Energies (in eV) of the $B_4O_2^-$ Anion, Compared with the Corresponding Theoretical Values at the OVGF(full) and CASPT2 Levels

			OVGF(full)[b]			
	transition	expt[a]	B3LYP	B3PW91	MP2	CASPT2
X	$^3\Sigma_g^- \leftarrow {}^2\Pi_u$	3.160 (15)	3.054 (0.895)	3.047 (0.895)	3.069 (0.895)	3.061
A	$^1\Delta_g \leftarrow {}^2\Pi_u$	3.64 (3)	3.322 (0.895)	3.315 (0.895)	3.336 (0.895)	3.521
B	$^1\Sigma_g^+ \leftarrow {}^2\Pi_u$	3.99 (3)	3.872 (0.900)[c]	3.865 (0.900)[c]	3.885 (0.899)[c]	3.929

[a] Numbers in parentheses represent experimental uncertainties in the last digits. [b] The numbers in parentheses indicate the pole strength, which characterizes the validity of the one-electron detachment picture. [c] The next detachment channel is calculated with a VDE (in eV) of 8.651 (0.843), 8.660 (0.843), and 8.610 (0.842) at B3LYP, B3PW91, and MP2 geometries, respectively. Pole strength is shown in parentheses.

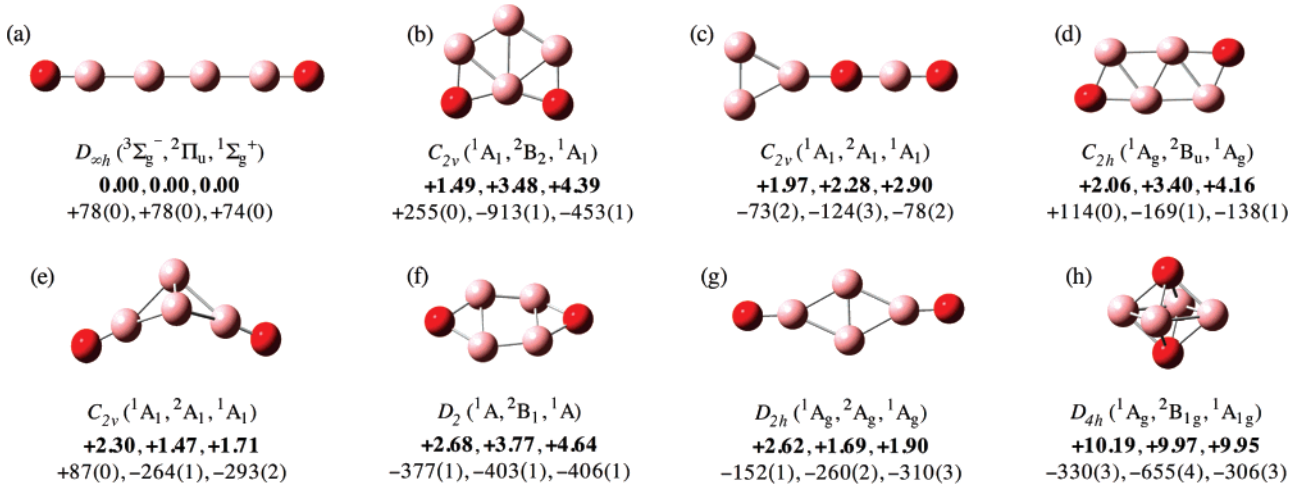

Figure 2. Optimized structures of B_4O_2, $B_4O_2^-$, and $B_4O_2^{2-}$ at the B3LYP level. Labeled below each structure are the symmetries and electronic states, relative energies in eV (bold), and the lowest vibrational frequencies (in cm^{-1}) for the neutral, anion, and dianion, respectively. The number in the parentheses of the lowest vibrational frequency is the imaginary frequencies.

pvtz, and CASPT2 levels and are compared with the experimental results in Table 1. The five levels of theory gave consistent values: ADE (3.06−3.12 eV) and VDE (3.12−3.17 eV). Vibrational frequencies of the totally symmetric modes of the $B_2(BO)_2$ neutral, at B3LYP, B3PW91, and MP2 levels, are also given in Table 1. Nearly identical frequencies were obtained at the three levels of theory. Vertical one-electron detachment energies of $B_2(BO)_2^-$ were also calculated at the OVGF(full) level using the anion structures at B3LYP, B3PW91, MP2, and also at the CASPT2 level, as shown in Table 2.

5. Comparison Between Experiment and Theory

5.1. Interpretation and Assignments of the PES Spectra. The global minimum linear structure of B_4O_2 possesses a triplet ground state ($^3\Sigma_g^-$), which is consistent with the PES pattern (no HOMO−LUMO gap). The computed structural changes between the neutral and anion are also very small (Figure 3), in agreement with the rather sharp ground state PES transition. As shown in Tables 1 and 2, the calculated detachment energies and vibrational frequencies are all in excellent agreement with

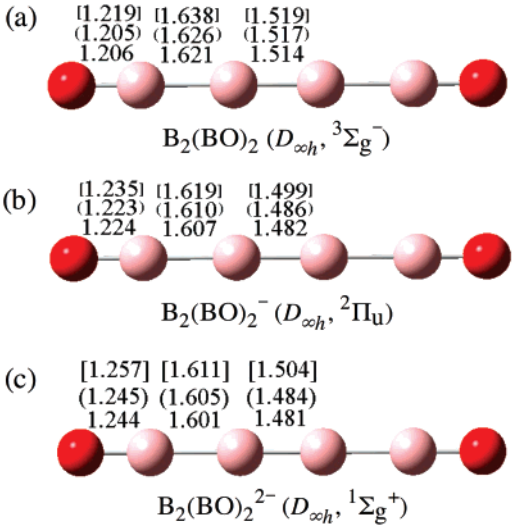

Figure 3. Optimized ground state structures of (a) $B_2(BO)_2$, (b) $B_2(BO)_2^-$, and (c) $B_2(BO)_2^{2-}$. The bond lengths (in Å) are labeled as B3LYP, (B3PW91), and [MP2] levels, respectively.

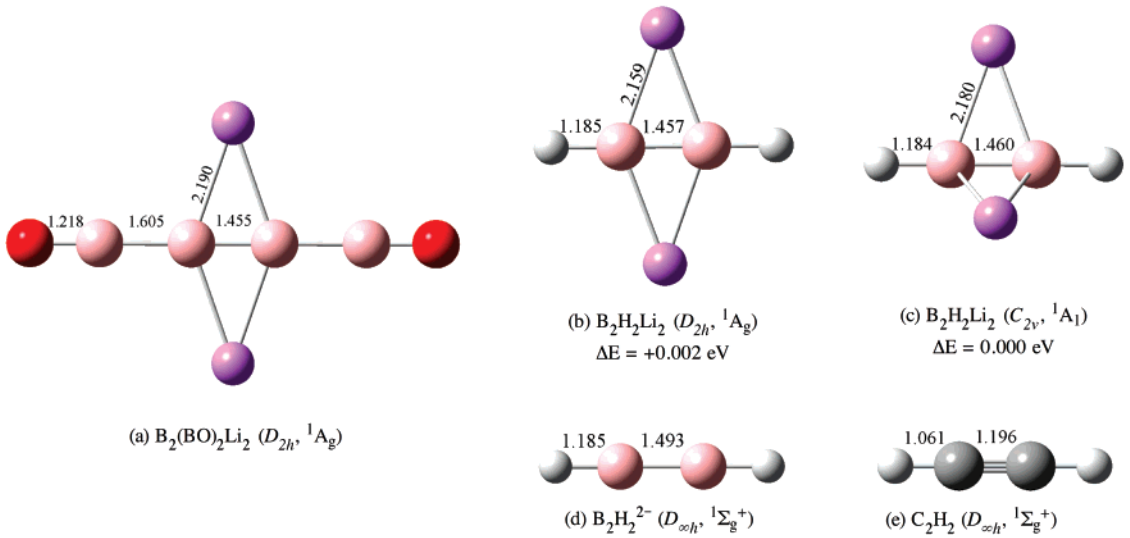

Figure 4. (a) Optimized ground state structure of $B_2(BO)_2Li_2$; (b and c) Two low-lying structures of $B_2H_2Li_2$ with their relative energies; (d) Ground state structure of $B_2H_2^{2-}$; and (e) Ground state structure of C_2H_2. All data are at the B3LYP level. Bond lengths are shown in Å.

the experimental results, lending considerable credence to the linear global minimum structure for B_4O_2 and $B_4O_2^-$.

The linear $B_2(BO)_2$ has an electronic configuration of $1\sigma_g^2 1\sigma_u^2 2\sigma_g^2 2\sigma_u^2 3\sigma_g^2 1\pi_u^4 1\pi_g^4 2\pi_u^2$ ($^3\Sigma_g^-$), where the $2\pi_u$ HOMO is half-filled, resulting in a triplet ground state. In $B_2(BO)_2^-$, the extra electron enters the half-filled $2\pi_u$ HOMO, yielding an electronic configuration of $1\sigma_g^2 1\sigma_u^2 2\sigma_g^2 2\sigma_u^2 3\sigma_g^2 1\pi_u^4 1\pi_g^4 2\pi_u^3$ ($^2\Pi_u$). One-electron detachment from the $2\pi_u^3$ HOMO will result in three closely lying electronic states: $^3\Sigma_g^-$, $^1\Delta_g$, and $^1\Sigma_g^+$, which should be responsible for the three PES bands (Table 2). The calculated ground state ADE (Table 1) is 3.119 eV (B3LYP), 3.066 eV (B3PW91), and 3.082 eV (MP2), which all agree well with the experimental value 3.160 eV. Because of the small geometry changes between the anion and neutral, the ADE and VDE were identical (both were measured from the 0−0 transition). The calculated ground state VDE (Table 1) is also very close to the calculated ADE, again consistent with the experimental observation.

OVGF calculations provide one-electron detachment energies for the ground and excited states of $B_2(BO)_2$. The OVGF method assumes that single determinants give a qualitatively reasonable description of the initial and final states in photodetachment detachments. In the current case, this assumption is not valid for the transition to the $^1\Sigma_g^+$ final state. For the transition to the $^1\Delta_g$ state, there are also multiconfigurational issues. However, as shown in Table 2, the OVGF calculations at the B3LYP, B3PW91, and MP2 geometries yielded surprisingly consistent detachment energies with quite large pole strengths for all detachment channels (0.84−0.90). In particular, the VDE for the next detachment channel was predicted by OVGF to be at 8.6 eV (see footnote c in Table 2), in perfect agreement with the absence of any PES bands beyond ∼4 eV in the 193 nm spectrum (Figure 1b). The CASPT2 results are in quantitative agreement with the experimental values. In particular, the VDE's for the first and second excited states were predicted to be 3.521 and 3.929 eV at CASPT2, in excellent agreement with the experimental VDE's of 3.64 and 3.99, respectively (Table 2).

5.2. Assignments of the Observed Vibrational Modes. The resolved vibrational frequencies in the 355 nm spectrum (Figure 1a) for the ground state transition provide highly valuable information for structural characterization. The vibrational frequencies of all the modes for the linear $B_2(BO)_2$ cluster are given in Table S2 at the B3LYP level of theory. Among the nine vibrational modes, there are three totally symmetric ones, which can be viewed as the B—B, B═B, and B≡O symmetric stretching in the linear O≡B—B═B—B≡O structure. Since only totally symmetric vibrational modes are allowed in photodetachment transitions, the number of allowed vibrational modes in the linear B_4O_2 cluster is consistent with the observed number of modes. The calculated frequencies for the three totally symmetric modes at B3LYP and B3PW91 are compared with the experimental observations in Table 1. The predicted frequency for the low-frequency B—B mode at all three levels of theory seems to be slightly high relative to the experimental value, whereas the predicted frequencies for the B═B and B≡O modes appear to be slightly low. The frequencies obtained from the PES experiments are not very accurate, in particular for the B—B mode, making it difficult to compare quantitatively with the theoretical predictions. Nevertheless, the overall agreement between the experiment and theory is satisfactory, allowing us to assign the 350, 1530, and 2040 cm^{-1} observed frequencies to the B—B, B═B, and B≡O symmetric stretching modes, respectively. The HOMO (π_u) of $B_2(BO)_2^-$ involves strong bonding interactions among the four central BBBB atoms with some slightly antibonding interactions in the terminal boronyl units (Table 3). This MO character is consistent with the observed vibrational activities in the PES spectrum and the calculated bond length changes from the anion to the neutral (Figure 3).

6. Discussion

6.1. Chemical Bonding in $B_2(BO)_2^{0/-/2-}$: Diboronyl Diborene. The B_4O_2 cluster can be viewed as a B_2 core bonded terminally with two boronyl groups. The BB bond length within the B_2 core is 1.514 Å at the B3LYP level (Figure 3a), suggesting double bond characters, whereas the BB bond length between the B_2 core and the BO groups is 1.621 Å, characteristic of B—B single bonds. The BO bond length is 1.206 Å, which is typical for a B≡O triple bond.[21,25,39] There is a systematic change of the bond lengths with charge states: the boronyl bond

Table 3. Selected Molecular Orbitals Which Are Mainly Responsible for the BB Multiple Bond within the B_2 Core and the Two BB Single Bonds between the B_2 Core and the Terminal BO Groups for $B_2(BO)_2$, $B_2(BO)_2^-$, and $B_2(BO)_2^{2-}$ [a]

	BB multiple bond		BB single bonds	
	π_u	σ_g	σ_u	σ_g
$B_2(BO)_2$ ($^3\Sigma_g^-$)	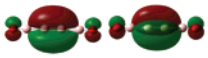 HOMO (*2*)	 HOMO–3 (*2*)	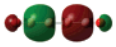 HOMO–6 (*2*)	 HOMO–7 (*2*)
$B_2(BO)_2^-$ ($^2\Pi_u$)	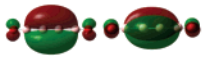 HOMO (*3*)	 HOMO–3 (*2*)	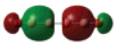 HOMO–6 (*2*)	 HOMO–7 (*2*)
$B_2(BO)_2^{2-}$ ($^1\Sigma_g^+$)	 HOMO (*4*)	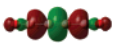 HOMO–1 (*2*)	 HOMO–6 (*2*)	 HOMO–7 (*2*)

[a] Shown in *italic* are the occupation numbers of the corresponding orbitals.

length increases slightly from $B_2(BO)_2$ to $B_2(BO)_2^{2-}$, whereas all the BB bond lengths decrease slightly from $B_2(BO)_2$ to $B_2(BO)_2^{2-}$ (Figure 3). The evolution of bond lengths and the chemical bonding with charge states in $B_2(BO)_2^{0/-/2-}$ can be readily understood through MO analyses.

The key bonding MO's that are responsible for the BB bonding within the B_2 core and the BB bonding between the B_2 core and the boronyl groups are shown in Table 3 for $B_2(BO)_2^{0/-/2-}$. A full analysis of all valent MO's is shown in Table S3. The combination of σ_u (HOMO-6) and σ_g (HOMO-7) in all three species can be localized as two B−B single bonds, which are responsible for the B−B σ-bonding between the B_2 core and the BO groups. These MO's can be traced back to the 3σ HOMO of the bare boronyl BO radical (Table S3). The single B−B bond can be easily recognized by the computed B−B bond length (1.621−1.601 Å).

The σ_g (HOMO-3) orbital can be considered to be responsible for the BB σ-bonding within the B_2 core (Table 3). The only difference among the three $B_2(BO)_2^{0/-/2-}$ species is the occupation of the HOMO, which is responsible for the BB π bonding within the B_2 core. In the neutral species the HOMO is half filled, and thus the BB bond can be considered to be a B═B double bond, as shown by the computed B═B bond distance of 1.514 Å, which is considerably shorter than the B−B single bond. Hence, the neutral $B_2(BO)_2$ cluster can be represented with the Lewis structure O≡B−B═B−B≡O. This bonding picture is consistent with Wiberg bond order analysis (Table 4).

The extra electrons successively occupy the degenerate π_u HOMO in $B_2(BO)_2^-$ and $B_2(BO)_2^{2-}$, respectively (Table 3). There is a slight decrease of the BB bond distance with the BB core in $B_2(BO)_2^-$, and this bond can be considered to have a bond order of 2.5. The increase of the bond order is borne out also in the Wiberg bond order analysis (Table 4). In $B_2(BO)_2^{2-}$, the HOMO is fully occupied, and the central BB bond can be considered to be of the bond order 3. The central BB bond length in $B_2(BO)_2^{2-}$ does not contract much in comparison to that in $B_2(BO)_2^-$. This effect is likely due to the coulomb repulsion in the dianion, in which each B atom at the center carries a natural atomic charge of −0.75 |e| (Table 4). The coulomb repulsion effect is confirmed in $B_2(BO)_2Li_2$ (Figure 4a), in which the central B≡B triple bond has a bond length of 1.455 Å, compared to 1.481 Å in $B_2(BO)_2^{2-}$. Thus, $B_2(BO)_2^{2-}$ can be legitimately considered as containing a triply bonded B_2 core with the Lewis structure, $[O{\equiv}B{-}B{\equiv}B{-}B{\equiv}O]^{2-}$, i.e., diboronyl diborene.

Table 4. Natural Atomic Charges of the Central B Atoms q_B(|e|) (q_C in C_2H_2) and the Li Atoms q_{Li}(|e|), Wiberg Bond Orders for BB Multiple (WBI) and Single Bonds (WBI_{B-B}), and the Total Bond Indices of the Central B Atoms (WBI_B) or WBI_C for C_2H_2

	q_B/q_C	q_{Li}	WBI	WBI_{B-B}	WBI_B/WBI_C
$B_2(BO)_2$	+0.02		1.44 (B═B)	1.07	2.57
$B_2(BO)_2^-$	−0.37		1.97 (B═/≡B)	1.14	3.27
$B_2(BO)_2^{2-}$	−0.75		2.43 (B≡B)	1.24	3.96
D_{2h}-$B_2(BO)_2Li_2$	−0.94	+0.96	2.61 (B≡B)	1.13	3.97
B_2H_2	+0.09		1.50 (B═B)		2.49
$B_2H_2^-$	−0.38		2.25 (B═/≡B)		3.24
$B_2H_2^{2-}$	−0.87		3.00 (B≡B)		4.00
D_{2h}-$B_2H_2Li_2$	−0.91	+0.94	2.90 (B≡B)		4.00
C_2H_2	−0.23		3.00 (C≡C)		3.95

6.2. On the B≡B Triple Bond in $B_2(BO)_2^{2-}$: Comparison with OCBBCO. BB multiple bonds are rare in chemistry. To our knowledge, the only previous report beyond the B═B double bond is that in OCBBCO prepared and identified in a low-temperature matrix by Zhou et al.[13] The current study shows that the $B_2(BO)_2^{2-}$ cluster is a novel chemical species with a rare B≡B triple bond. In fact, $B_2(BO)_2^{2-}$ is isoelectronic with the $B_2(CO)_2$ molecule by Zhou et al. However, there are some significant differences between $B_2(BO)_2^{2-}$ and $B_2(CO)_2$. First of all, OCBBCO was characterized as a metastable species and readily underwent photochemical rearrangement to form OBBCCO and OBCCBO, which are ∼2.6 and ∼4.1 eV more stable, respectively, at the B3LYP level.[18] The $B_2(BO)_2^{2-}$ species, on the other hand, represents a true global minimum. Second and more interestingly, the calculated Wiberg bond order in OCBBCO is $WBI_{B\equiv B}$ = 1.97, which is comparable to that in $B_2(BO)_2^-$ ($WBI_{B\equiv B}$ = 1.97). This is because of the fact that the triple bond character in OCBBCO comes from the back-donation from the terminal carbonyl group.[13] Thus, the BB bond order in OCBBCO may be more appropriately characterized as 2.5, resulting in the $B_2(BO)_2^{2-}$ species being the first molecule with a true B≡B triple bond ($WBI_{B\equiv B}$ = 2.43, Table 4).

6.3. On the Key Structural Role of the Boronyl Groups in $B_2(BO)_2^{0/-/2-}$. One of the most interesting features of small boron clusters is their multicenter bonding with aromatic and antiaromatic characters.[5,6] The $B_4^{+/0/-/2-}$ clusters are known to

be aromatic with rhombus structures.[6,39] However, upon oxidation the B_4 motif appears to be completely destroyed in $B_2(BO)_2^{0/-/2-}$. The structure and bonding in $B_2(BO)_2^{0/-/2-}$ seem to be mainly governed by the presence of the boronyl groups with localized classical bonding. In our recent work on the $B_3O_2^-$ and $B_4O_3^-$ clusters, we showed for the first time the major role that the boronyl groups play in oxygen-poor boron oxide clusters, yielding a linear $B(BO)_2^-$ ($D_{\infty h}$) and triangular $B(BO)_3^-$ (D_{3h}) structure, respectively.[25] A recent DFT study on a series of oxygen-deficient B_mO_n clusters also revealed the presence of BO groups.[29] The BO bond length in $B_2(BO)_2$ is calculated to be 1.21 Å (Figure 3), which is remarkably similar to 1.203 Å in free BO radical[21] and 1.209/1.203 Å in $B(BO)_2$/$B(BO)_3$ at the B3LYP level,[25] again demonstrating the structural robustness of the boronyl groups in boron oxide clusters.

The boronyl groups act as monovalent σ-donor ligands in $B_2(BO)_2^{0/-/2-}$, as well as in $B(BO)_2^-$ and $B(BO)_3^-$.[25] Thus, the BO group can be viewed as isovalent to the H atom, suggesting an interesting link between the boron oxide clusters and boron hydrides. Indeed, the neutral $B_2(BO)_2$ cluster displays quite similar bonding and electronic structure to the linear diborene B_2H_2, which also has a triplet $^3\Sigma_g^-$ ground state.[12] The $B_2(BO)_2^{2-}$ dianion is analogous to $B_2H_2^{2-}$, as shown in Figure 4d. The latter is isoelectronic to C_2H_2, and its triple B≡B bond length (1.493 Å at B3LYP) is also very similar to that in $B_2(BO)_2^{2-}$ (Figure 3c).

The stability of $B_2(BO)_2^{2-}$ suggests that it may serve as a new building block in bulk compounds. We tested this possibility by considering the neutral complex, $B_2(BO)_2Li_2$, as shown in Figure 4a. We found that the Li atom donates its charge to the $B_2(BO)_2$ core, with very little structural distortion. It can be essentially viewed as $Li^+[B_2(BO)_2^{2-}]Li^+$ with predominantly ionic interactions. The compensation of the coulomb repulsion within the dianion core by the Li^+ counterion reduces the B≡B triple bond length. Hence, we observe a perfect correlation between the BB multiple bond order and its bond length in the neutral $B_2(BO)_2 \rightarrow B_2(BO)_2^- \rightarrow B_2(BO)_2Li_2$: 2 (1.514 Å) → 2.5 (1.482 Å) → 3 (1.455 Å). If it can be synthesized in bulk, the $B_2(BO)_2^{2-}$ species would be the first boron compound with a B≡B triple bond.

7. Conclusions

Vibrationally resolved photoelectron spectra are reported for $B_4O_2^-$ at 355 and 193 nm, yielding an accurate electron affinity for neutral B_4O_2 as 3.160 ± 0.015 eV. Three detachment bands were observed in the 193 nm spectrum at 3.16, 3.64, and 3.99 eV. The 355 nm spectrum revealed three vibrational modes for the ground state of B_4O_2: 350 ± 40, 1530 ± 30, and 2040 ± 30 cm^{-1}. Extensive theoretical calculations were performed on $B_4O_2^{0/-}$, which were found to possess highly stable linear ground state structures, OBBBBO ($D_{\infty h}$, $^3\Sigma_g^-$), and $OBBBBO^-$ ($D_{\infty h}$,$^2\Pi_u$). Excellent agreement is obtained between the calculated electron detachment energies and vibrational frequencies and the experimental observations, firmly establishing the linear global minimum structures for $B_4O_2^{0/-}$. Molecular orbital analyses showed that the B_4O_2 cluster can be described as O≡B−B═B−B≡O, i.e., a double bonded B_2 core terminally coordinated with two boronyl groups. The observed vibrational frequencies, 350, 1530, and 2040 cm^{-1}, agree well with the calculated B−B, B═B, and B≡O symmetric stretching vibrations, respectively. Chemical bonding analyses suggest that the bond order within the B_2 core increases from 2 to 2.5 from $B_2(BO)_2$ to $B_2(BO)_2^-$, culminating with a true B≡B triple bond in $B_2(BO)_2^{2-}$, i.e., $[O{\equiv}B{-}B{\equiv}B{-}B{\equiv}O]^{2-}$ (diboronyl diborene). The high electronic and structural stability of $B_2(BO)_2^{2-}$ suggests that it may be synthesized in an ionic salt, such as in the form of $B_2(BO)_2Li_2$, and would be the first boron compound containing a B≡B triple bond. The current work demonstrates again the importance of the boronyl groups as a key structural unit in boron oxide clusters and may open the way to designing many novel boronyl compounds.

Acknowledgment. This work was supported by the National Science Foundation (DMR-0503383) and performed at EMSL, a national scientific user facility sponsored by the DOE's Office of Biological and Environmental Research and located at the Pacific Northwest National Laboratory, operated for the DOE by Battelle. S.D.L. gratefully acknowledges financial support from the National Natural Science Foundation of China (No. 20573088 and No. 20743004).

Supporting Information Available: Cartesian coordinates optimized at the B3LYP level for $B_2(BO)_2^{0/-/2-}$, $B_2(BO)_2Li_2$, $B_2H_2^{2-}$, and C_2H_2; vibrational frequencies of $B_2(BO)_2$ at the B3LYP level; bonding MO's of $B_2(BO)_2$, $B_2(BO)_2^-$, $B_2(BO)_2^{2-}$, and $B_2(BO)_2Li_2$ as compared with those of the BO boronyl radical; and complete ref 35. This material is available free of charge via the Internet at http://pubs.acs.org.

JA0771080